Research Square

Preprints are preliminary reports that have not undergone peer review.
They should not be considered conclusive, used to inform clinical practice,
or referenced by the media as validated information.

African Swine Fever Virus pI10L Enhances Antiviral Immune Responses by Promoting MAVS-TRAF6 Signaling

Jiaona Guo
Nanjing Agricultural University
Jiaxuan Lv
Nanjing Agricultural University
Yongxin Hu
China Animal Health and Epidemiology Center
Huan Chen
Nanjing Agricultural University
Xiaoyu Gao
Nanjing Agricultural University
Shengqiang Ge
China Animal Health and Epidemiology Center
Jinming Li
China Animal Health and Epidemiology Center
Yong-Sam Jung
Nanjing Agricultural University
Xiaodong Wu
China Animal Health and Epidemiology Center
Yingjuan Qian
yqian@njau.edu.cn

Nanjing Agricultural University

Research Article

Keywords: African swine fever virus, innate immune responses, pI10L, MAVS, TRAF6

Posted Date: September 1st, 2026

DOI: https://doi.org/10.21203/rs.3.rs-10742481/v1

License: This work is licensed under a Creative Commons Attribution 4.0 International License.
Read Full License

Additional Declarations: No competing interests reported.

Abstract

African swine fever (ASF) is a highly contagious and lethal viral disease that affects both domestic and wild pigs. The ASF virus (ASFV) encodes multiple immune evasion proteins that help it circumvent host adaptive immunity; however, the intricate host-pathogen interactions remain incompletely characterized, hindering the development of effective vaccines. In this study, we identified the ASFV pI10L as a positive regulator of the innate immune response. Specifically, we demonstrated that pI10L interacted with the mitochondrial antiviral-signaling protein (MAVS) within critical innate immune pathways, promoting MAVS aggregation and the recruitment of downstream TRAF6, which in turn enhanced the antiviral response. Moreover, pI10L increased TRAF6 stability by inhibiting its K48-linked ubiquitination, thereby potentiating TRAF6-mediated NF-κB activation. Knockdown of *MAVS* or *TRAF6* attenuated the pI10L-mediated promotion of interferon-beta (IFN-β) and interleukin-6 (IL-6) production. Additionally, *I10L* knockdown in ASFV-infected primary porcine alveolar macrophages (PAMs) reduced IFN-β production and promoted viral replication, whereas ectopic expression of pI10L produced the opposite effect. Together, these findings uncover a novel role for pI10L in promoting antiviral immune responses and offer new insights into the complex interplay between ASFV and host innate immunity.

Introduction

African swine fever (ASF) is a highly contagious and lethal viral disease caused by the African swine fever virus (ASFV), which poses a significant threat to the pig farming industry [1]. Currently, there are no commercially available vaccines or antiviral therapeutics against ASFV. ASFV belongs to the *Asfarviridae* family and is a large, complex double-stranded DNA (dsDNA) virus with a linear genome ranging from 170 to 193 kilobase pairs [2, 3]. The ASFV genome contains 150 to 200 open reading frames (ORFs) that encode over 150 structural and nonstructural proteins involved in virus assembly, replication, and evasion of the host immune response [3, 4]. However, the functions of many ASFV genes remain uncharacterized, which poses a major challenge for the development of effective ASF vaccines. Therefore, investigating the roles of ASFV genes in immune regulation is crucial for advancing vaccine research.

Innate immune responses constitute the host's first line of defense against invading pathogens and help to limit their spread [5]. Upon viral infection, viral components or replication intermediates can be detected by various pattern recognition receptors (PRRs), which activate the antiviral innate immune response [5, 6]. PRRs include Toll-like receptors (TLRs), RIG-I-like receptors (RLRs), nucleotide-binding oligomerization domain (NOD)-like receptors (NLRs) and cytosolic DNA sensors such as cyclic GMP-AMP synthase (cGAS) [7, 8]. RLRs, comprising retinoic acid-inducible gene I (RIG-I), melanoma differentiation-associated gene 5 (MDA5), and laboratory of genetics and physiology 2 gene (LGP2), primarily recognize cytosolic RNAs [9, 10]. It has been demonstrated that RIG-I recognizes 5´-triphosphate poly-U/A-rich single-stranded RNA and short double-stranded RNA (dsRNA), whereas MDA5 binds to long dsRNA [11]. Additionally, RIG-I can detect the transcriptional products of RNA polymerase III that use AT-rich double-stranded DNA as a template [12]. Upon recognition of viral RNAs, RIG-I and

MDA5 are recruited to the adaptor protein mitochondrial antiviral signaling (MAVS) (also known as VISA, CARDIF, or IPS-1), which contains of an N-terminal CARD domain, a proline-rich region, and a C-terminal transmembrane (TM) domain [13–16]. Subsequently, MAVS rapidly forms large prion-like aggregates and recruits tumor necrosis factor receptor-associated factors (TRAFs, including TRAF2/3/5/6), serving as a platform for the assembly of the MAVS signalosome. The MAVS signalosome further recruits TBK1 and IκB kinase (IKKi) to activate interferon regulatory factors (IRF3/7) and nuclear factor κB (NF-κB) leading to the production of IFNs and proinflammatory cytokines [17–19]. Secreted type I interferons bind to interferon receptors (IFNAR) and activate the Janus Kinase (JAK)/Signal Transducer and Activator of Transcription (STAT) signaling pathway, thereby inducing the transcription of a battery of antiviral interferon-stimulated genes (ISGs) [20, 21].

TRAF6 plays an essential role in multiple pattern recognition receptor (PRR) signaling pathways [22]. Within the RLR pathway, the aggregation of MAVS provides a stable platform for recruiting TRAF family proteins. This recruitment facilitates TRAF oligomerization, which subsequently activates their intrinsic E3 ubiquitin ligase function [23]. As an E3 ubiquitin ligase, TRAF6 mediates Lys63-linked polyubiquitination of both itself and IκB kinase γ (IKKγ also known as NEMO) [24, 25]. The subsequent recruitment of the TAK1-TAB2-TAB3 complex to TRAF6 promotes TAK1-mediated activation of the IKK complex, ultimately inducing NF-κB activation and proinflammatory cytokine expression [26, 27]. Interestingly, TRAF6 can also activate IRF3 and induce IFNs production during viral infection [23]. Moreover, TRAF6 can function redundantly with TRAF2/5 to promote the activation of both IRF3 and IKK through additional, more complex mechanisms [23].

As a large DNA virus, ASFV readily activates the cGAS-STING pathway. However, previous studies have demonstrated that the AT-rich islands within the ASFV genome can convert dsDNA into dsRNA via RNA polymerase III, thereby triggering the RIG-I-mediated innate immune response [28]. In recent years, multiple ASFV-encoded proteins have been identified that evade host innate immune responses by inhibiting the production of type I IFNs and inflammatory cytokines. For example, ASFV proteins C129R and EP364R interact with cGAS and cleave 2',3'-cyclic GMP-AMP (cGAMP), thereby disrupting the cGAS-STING signaling pathway and inhibiting interferon (IFN) responses [29]. Similarly, pMGF505-6R mediates the degradation of STING via the proteasomal pathway, consequently impairing type I interferon production [30]. In the RLR pathway, ASFV pI267L antagonizes the RNA Pol-III-RIG-I axis by impairing Riplet-mediated activation of RIG-I [28]. Additionally, ASFV pS183L impairs RLR antiviral signaling by blocking MDA5 oligomerization [31], while pMGF360-4L inhibits interferon signaling by inducing the autophagy-dependent degradation of MDA5 [32]. Furthermore, ASFV pE248R blocks RIG-I signaling by targeting RIG-I and TRIM25 [33]. Beyond interferon inhibition, ASFV also targets inflammatory signaling; for instance, ASFV pD345L antagonizes NF-κB signaling by inhibiting IKKα/β kinase activity [34]. ASFV A238L suppresses NF-κB activation and the production of inflammatory cytokines by inhibiting the activation of p300. In contrast, another study demonstrated that A238L activates the TBK1-IRF3 signaling axis, thereby inducing the expression of interferon-β (IFN-β) and interferon-stimulated genes (ISGs) [35, 36].

The pI10L is a 170-amino-acid product of the *I10L* open reading frame (ORF), which is located in the right-variable region of the African swine fever virus (ASFV) genome. The *I10L* ORF shares homology with the *KP177R* gene, which encodes the p22 protein [3, 37]. Recent studies indicate that the ASFV pI10L inhibits the tumor necrosis factor-α (TNF-α)-mediated nuclear factor-κB (NF-κB) signaling pathway by suppressing IKKβ phosphorylation and the K63-linked ubiquitination of NEMO [38]. However, it remains unclear whether pI10L affects the production of type I interferon during ASFV infection.

In this study, we demonstrate for the first time that ASFV pI10L acts as a positive regulator of MAVS-mediated antiviral innate immunity. We show that ASFV pI10L enhances type I IFN production. Mechanistically, ASFV pI10L interacts with MAVS to promote its oligomerization and the subsequent recruitment of TRAF6, thereby facilitating the production of type I IFN and inflammatory cytokines. Consistent with these findings, knockdown of *I10L* in the parental ASFV strain attenuated the host innate immune response and increased viral replication. Our findings reveal that pI10L stimulates host antiviral immunity, providing crucial insights into the complex immune interactions of ASFV.

Results

ASFV pI10L enhances the poly(I:C)-mediated expression of antiviral genes.

To investigate the role of ASFV pI10L in innate antiviral immunity, we examined its effect on the expression of type I IFNs and antiviral genes. PK-15 cells were transfected with the ASFV *I10L* expression plasmid and subsequently stimulated with the dsRNA mimic ploy(I:C)-LMW/HMW (Low or high molecular weight) or the dsDNA mimic poly(dA:dT) to activate innate immune pathways. Quantitative RT-PCR (qRT-PCR) revealed that pI10L significantly enhanced the transcriptional activation of *IFN-β* induced by poly(I:C) (Fig. 1A). To further assess the impact of pI10L on downstream antiviral signaling, we measured the transcript levels of several proinflammatory cytokines and interferon-stimulated genes (ISGs) following poly(I:C)-HMW stimulation. As shown in Figs. 1B-E, overexpression of pI10L promoted the poly(I:C)-induced expression of *ISG56*, *ISG54*, *TNF-α* and *IL6*. We then evaluated the effect of pI10L on the phosphorylation levels of key signaling molecules by Western blot analysis. The results demonstrated that pI10L upregulated the poly(I:C)-induced phosphorylation of TBK1, IRF3, IκBα and p65 (Fig. 1F). Taken together, these findings define the ASFV pI10L as a potent promoter of the type I interferon (IFN-I) production pathway.

ASFV pI10L interacts with MAVS and TRAF6

The dsRNA mimic poly(I:C) is known to activate the RIG-I/MDA5-MAVS signaling pathway [39]. To further elucidate the molecular mechanisms by which pI10L positively regulates the antiviral immune response, we sought to identify its target signaling molecules within the RLR pathway. 293T cells were co-transfected with Flag-pI10L and HA-tagged signaling molecules, including RIG-I, MDA5, MAVS, TBK1, IRF3, and TRAF6, followed by co-immunoprecipitation (co-IP) assays using anti-Flag antibodies. The results showed that ASFV pI10L interacts with MAVS and TRAF6 (Figs. 2A-E and G). These interactions

were further confirmed by reverse co-IP using anti-HA antibodies (Figs. 2F and H). To determine whether pI10L interacts with MAVS and TRAF6 under physiological conditions, endogenous co-IP assays were performed in PK-15 cells, which demonstrated that pI10L binds to both MAVS and TRAF6 (Fig. 2I). Additionally, GST pull-down assays further confirmed that pI10L directly interacts with MAVS and TRAF6 in vitro (Figs. 2J and K). Collectively, these findings suggest that ASFV pI10L directly interacts with both MAVS and TRAF6.

MAVS comprises three domains: an N-terminal CARD domain that interacts with RIG-I or MDA5, a middle proline-rich region involved in protein-protein interactions, and a C-terminal transmembrane (TM) domain essential for anchoring MAVS to the mitochondrial outer membrane [13–16]. MAVS also contains three TRAF-interacting motifs (TIMs) required for binding TRAF2/3/5/6 and activating downstream signaling [16, 19, 23]. To identify which region of MAVS are responsible for binding with pI10L, we constructed five truncated mutants (aa1 to 336, aa101 to 524, aa101 to 336, aa336 to 498 and aa336 to 524). When each construct was co-expressed with pI10L and subjected to co-IP, we found that the full-length and the truncated forms (aa101 to 524, aa336 to 498 and aa336 to 524) of MAVS interacted with pI10L, whereas the truncated forms (aa1 to 336 and aa101 to 336) of MAVS lost the ability to interact with pI10L (Fig. 2L). Notably, the full-length and truncated forms (aa101 to 524 and aa336 to 524) of MAVS, all of which contain the TM domain, interacted with ASFV pI10L. These findings indicate that the TM domain of MAVS is essential for its binding to pI10L. Additionally, the truncated form (aa336 to 498) contains the TIM3 motif (aa445 to 450, PEENEY), which mediates the interaction between MAVS and TRAF6. These results suggest that ASFV pI10L may affect the interaction between MAVS and TRAF6.

TRAF6 comprises four major domains: an N-terminal RING finger domain, zinc finger domains, a coiled-coil domain (also known as the TRAF-N domain), and a TRAF-C domain [40]. Since pI10L binds to TRAF6, we sought to determine which domain of TRAF6 is required for this interaction. Accordingly, we constructed plasmids expressing four truncations of TRAF6 (Fig. 2M), as described previously [41], and detected their interaction with pI10L. Co-IP assays showed that pI10L interacted with wild-type (WT) TRAF6, the RING domain, and the TRAF-C domain, but not with the zinc figure and coiled-coil domains (Fig. 2M). These results suggest that MAVS and TRAF6 may serve as potential targets for ASFV pI10L in the regulation of interferon production.

ASFV pI10L facilitates MAVS aggregation and enhances its association with TRAF6

MAVS function is regulated by post-translational mechanisms, with ubiquitination and phosphorylation playing the most important roles in modulating its activity [42]. Upon viral infection, K63-linked ubiquitination of MAVS on the mitochondrial outer membrane induces its prion-like aggregation, a hallmark of MAVS activation [14, 42]. We next determined whether pI10L affects MAVS ubiquitination. As shown in Fig. 3A, co-IP assay results indicated that the pI10L protein did not affect MAVS ubiquitination. We then investigated whether pI10L modulates the formation of MAVS aggregates. Semidenaturing

detergent agarose gel electrophoresis (SDD-AGE) assays showed that ASFV pI10L facilitated the prion-like aggregation of MAVS (Fig. 3B). These results suggest that the pI10L modulates MAVS-mediated antiviral signaling by facilitating its aggregation.

Upon aggregation, MAVS acts as a central platform for recruiting downstream signaling molecules such as TRAF2/3/5/6, TBK1, and IRF3, which in turn induce the expression of antiviral genes [43–45]. Consistently, co-IP assays demonstrated that pI10L promoted the recruitment of TRAF6 to the MAVS complex (Fig. 3C). We further investigated whether pI10L promotes the interaction between MAVS and TRAF6 in a dose-dependent manner. The results confirmed that the pI10L protein facilitated TRAF6 recruitment to MAVS in a dose-dependent fashion (Fig. 3D). These results suggest that the pI10L strengthens the innate antiviral response by promoting the assembly of TRAF6 into the MAVS signaling complex.

ASFV pI10L inhibits the K48-linked polyubiquitination of TRAF6

TRAF6 consists of four major structural domains: an N-terminal RING finger domain, Zinc figure domains, a Coiled-coil domain and a TRAF-C domain [40]. The RING domain functions as an E3 ubiquitin ligase that mediates TRAF6 self-ubiquitination [46]. The TRFAF-C domain is responsible for protein-protein interactions, including those with upstream regulators and downstream effectors [47]. We have previously demonstrated that ASFV pI10L interacts with the RING domain of TRAF6. Therefore, we next determined whether pI10L affects the ubiquitination of TRAF6. Using a ubiquitination assay, we found that pI10L inhibited TRAF6 ubiquitination, specifically resulting in a significant decrease in K48-linked ubiquitination (Figs. 4A and B).

K48-linked polyubiquitination is well established as a signal targeting proteins for degradation by the 26S proteasome [48, 49]. To investigate the effect of pI10L on TRAF6 stability, PK-15 cells were co-transfected with plasmids expressing HA-pI10L and HA-TRAF6, and then subjected to Western blot assays. The results showed that pI10L increased the protein level of TRAF6 in dose-dependent manner (Fig. 4C). Together, our findings demonstrate that the ASFV pI10L enhances TRAF6 stability by specifically inhibiting K48-linked ubiquitination.

Previous studies have identified that the ASFV pI10L protein inhibits the TNFα-mediated NF-κB signaling pathway by suppressing IKKβ phosphorylation and the K63-linked ubiquitination of NEMO [38]. To further investigate its functional role, we assessed the effect of pI10L on NF-κB promoter activity in 293T cells. Interestingly, ectopic expression of pI10L promoted NF-κB promoter activation induced by TRAF6 but not by TAK1/TAB1 or p65 (Fig. 4E and G). Consistent with previous reports, pI10L inhibited NF-κB promoter activation mediated by IKKβ (Fig. 4F). Collectively, these results suggest that ASFV pI10L positively modulates NF-κB activation within the context of TRAF6 signaling, likely through its inhibition of K48-linked polyubiquitination and thereby stabilizing TRAF6.

pI10L mediates MAVS/TRAF6-dependent IFN-β production and modulates ASFV replication in porcine macrophages

To confirm that ASFV pI10L promotes IFN-β induction primarily by targeting MAVS and TRAF6, PK-15 cells were transfected with *MAVS* or *TRAF6*-specific siRNA for 48 hours, which effectively reduced the corresponding protein levels (Figs. 5A and D). Subsequent experiments demonstrated that knockdown of *MAVS* or *TRAF6* significantly suppressed poly(I:C)-induced *IFN-β* and *IL6* mRNA expression (Figs. 5B, C, E, and F). Notably, the knockdown of either *MAVS* or *TRAF6* also diminished the enhancing effect of pI10L on poly(I:C)-induced *IFN-β* and *IL-6* transcription (Figs. 5B, C, E, and F). Together, these findings demonstrate that ASFV pI10L enhances IFN-β and IL-6 production in a MAVS/TRAF6-dependent manner.

To further investigate the role of ASFV pI10L in interferon production during ASFV infection, we knocked down *I10L* expression in primary porcine alveolar macrophage (PAM) cells using two siRNAs specifically targeting the *I10L* transcript. PAMs were transfected with either negative control siRNAs (siNC) or siRNAs targeting *I10L* (siI10L) for 24 hours, followed by mock infection or infection with ASFV for 36 hours. Subsequently, the mRNA expression levels of *I10L*, *IFN-β*, *CP204L* (p30), and *B646L* (p72) were quantified using qRT-PCR. The qRT-PCR analysis confirmed effective silencing of *I10L* (Fig. 6A). Upon ASFV infection, *I10L*-knockdown cells exhibited lower *IFN-β* mRNA levels than siNC-treated cells (Fig. 6B). Consistently, knockdown of *I10L* increased the transcription of the viral genes *B646L* (p72) and *CP204L* (p30) (Figs. 6C and D). Western blot analysis further showed increased levels of p72 and p30 proteins in *I10L*-knockdown cells compared with siNC controls after infection (Fig. 6E). Conversely, pI10L overexpression in PAMs produced the opposite effects, reducing viral gene expression and enhancing *IFN-β* production (Figs. 6F-H). Consistent with the qRT-PCR results, Western blot analysis also showed that the expression of pI10L downregulated the protein levels of ASFV p72 and p30 (Fig. 6G). Taken together, these results demonstrate that the pI10L protein induces IFN-β production during ASFV infection.

Discussion

The innate immune response serves as the host's first line of defense against invading pathogens, limiting their spread [5]. Upon viral infection, various pattern recognition receptors recognize pathogen-associated molecular patterns, leading to the activation of innate immune signaling pathways and the subsequent production of type I interferons (IFN-I) [50, 51]. ASFV is a large, enveloped, double-stranded DNA (dsDNA) virus [2], is known to predominantly activate the cGAS-STING signaling pathway. To subvert host immunity, ASFV encodes multiple proteins that inhibit IFN-I production by antagonizing cGAS-STING signaling. Previous studies have also demonstrated that the AT-rich genomic DNA of ASFV can trigger innate antiviral responses through the RNA Pol III–RIG-I pathway [28]. Therefore, we hypothesized that ASFV may encode proteins that modulate the RLR signaling pathway. In this study, we found that the ASFV pI10L protein enhances IFN production induced by the dsRNA mimic poly(I:C) and promotes the phosphorylation of key signaling molecules in the innate immune cascade (Fig. 1). Given

that transfection of poly(I:C) activates the RLR pathway, our results suggest that pI10L may play a regulatory role in RLR-mediated innate immunity.

The mitochondrial antiviral signaling protein (MAVS) is a key adaptor in the RIG-I-like receptor (RLR) signaling cascade [42]. Upon viral infection, RIG-I and MDA5 interact with MAVS, which subsequently MAVS forms prion-like aggregates to activate the type I interferon signaling [52]. To evade host antiviral innate immunity, viruses have evolved diverse strategies to target the MAVS protein. During JEV infection, the NS1 protein upregulates miR-22, leading to downregulation of MAVS and consequent impairment of type I IFN production [53]. FMDV VP3 suppresses the type I IFN response by targeting the MAVS TM domain and inhibiting its key functions-mitochondrial localization, self-association, and aggregation [54]. In this study, we found that ASFV pI10L interacts with MAVS (Fig. 2). The prion-like aggregation of MAVS is essential for its activation; this process is thought to relieve the autoinhibition mediated by its C-terminal domain (approximately aa 360–540) following viral infection [55, 56]. We identified the MAVS region (aa 336–524) required for pI10L binding, implicating pI10L in the regulation of type I IFN production through modulation of MAVS prion-like aggregation. Further studies suggested that the ASFV I10L protein promotes the formation of MAVS aggregates (Fig. 3). These aggregates serve as signaling platform that recruit downstream components such as TRAF2/3/5/6, TBK1, and IKK, ultimately activating the antiviral immune response [17–19]. Additionally, ASFV pI10L protein increased the interaction between MAVS and TRAF6 (Fig. 3). How ASFV pI10L controls its promoting effect on MAVS aggregation and activation deserves further investigation.

TRAF6 is a critical signaling adaptor involved in NF-κB activation and multiple pattern recognition receptor pathways [22]. MAVS interacts with TRAF2 or TRAF6 to mediate IKK-dependent NF-κB activation and with TRAF3 to specifically activate the TBK1-dependent IRF3 pathway [57]. Here, we found that ASFV pI10L promotes TRAF6-mediated activation of the NF-κB promoter in 293T cells (Fig. 4D). We also found that pI10L directly binds to TRAF6, specifically its RING and TRAF-C domains (Fig. 2M). Since the RING domain confers E3 ubiquitin ligase activity to TRAF6 [58], we investigated whether pI10L modulates its ubiquitination. Our results showed that pI10L enhances TRAF6 protein stability by suppressing K48-linked polyubiquitination (Figs. 4A and B). Interestingly, a previous study reported that pI10L inhibits TNFα-induced NF-κB signaling by suppressing IKKβ phosphorylation and K63-linked ubiquitination of NEMO [38]. In line with this, we also observed that pI10L suppresses IKKβ-mediated NF-κB promoter activation (Fig. 4F). Given that IKKβ is a downstream component of TRAF6 signaling, the mechanism by which pI10L promotes TRAF6-mediated NF-κB activation-despite inhibiting IKKβ-remains unresolved and suggests a more complex mode of regulation.

In this study, we observed that ectopic expression of pI10L suppressed ASFV replication, whereas knockdown of pI10L in ASFV-infected porcine alveolar macrophages (PAMs) led to increased viral replication (Fig. 6). These results collectively suggested that ASFV pI10L plays a critical role during viral replication. Additionally, the data suggested that pI10L can induce IFN production, thereby activating the host antiviral response.

In summary, our study identified ASFV pI10L as a positive regulator of the innate immune response. We demonstrate that the ASFV pI10L interacts with MAVS to promote its aggregation and the subsequent recruitment of TRAF6, thereby activating the antiviral response. Furthermore, pI10L enhances TRAF6-mediated NF-κB signaling by inhibiting K48-linked ubiquitination, which stabilizes the TRAF6 protein (Fig. 7). Additionally, knockdown of pI10L inhibits the transcription of *IFN-β* and *IL6* in ASFV-infected PAMs. Collectively, these findings provide novel insights into the intricate interplay between ASFV and host innate immunity.

Materials and methods

Cell culture and virus

293T cells and porcine kidney (PK-15) cells were cultured in Dulbecco's modified Eagle's medium (DMEM; Invitrogen, Carlsbad, CA, USA) supplemented with 8% fetal bovine serum (PAN Biotech, Aidenbach, Germany) and 1% penicillin and streptomycin (Beyotime Biotechnology, Shanghai, China) at 37°C with 5% CO_2. PAM cells were grown in RPMI 1640 medium (BasalMedia, Shanghai, China) supplemented with 10% fetal bovine serum and 1% penicillin and streptomycin.

The ASFV China/LN/2018/1 strain (GenBank accession number OP856591.1, abbreviated as ASFV-CN2018), utilized in this study, was preserved by the China Animal Health and Epidemiology Center (CAHEC) in Shandong province, China.

Plasmids, antibodies and reagents

The *I10L* gene was amplified from the genomic DNA (gDNA) of the ASFV SY18 strain (GenBank No. MH766894.3) and cloned into pCAGGS-N-Flag, pCAGGS-N-HA, or pGEX-4T-1 vectors, generating pFlag-pI10L, pHA-pI10L, or pGST-pI10L, respectively. Plasmids expressing HA-tagged pig RIG-I, MDA5, MAVS, TBK1, IRF3, and TRAF6 were constructed as previously described [34, 59]. The NF-κB firefly luciferase reporter and pCMV-RL Renilla luciferase reporter plasmids have been described previously [59].

The antibodies used in this study and their sources were as follows: Mouse anti-Flag antibody was purchased from Sigma-Aldrich (St. Louis, MO, USA). Rabbit anti-TRAF6 (sc-7221) antibody was from Santa Cruz Biotechnology. Rabbit anti-MAVS (3993S), anti-phospho-TBK1 (S172, 5483S), anti-phospho-IκBα (2859S), anti-IRF3 (4302S), anti-NF-κB p65 (8242P), anti-phospho-NF-κB p65 (3033S) antibodies were from Cell Signaling Technology (Danvers, MA, USA). Rabbit anti-phospho-IRF3 (Ser396, #AF2436) antibody was from Affinity Biosciences (Cincinnati, OH, USA). Rabbit anti-HA (51064-2-AP) antibody and Mouse anti-TBK1 (67211-1), anti-IκBα antibodies were from Proteintech (Chicago, IL, USA). HRP-conjugated goat anti-mouse IgG (H + L) or anti-rabbit IgG (H + L) were purchased from Millipore (Burlington, MA, USA).

Poly(dA:dT), high molecular weight (HMW) poly(I:C) and low molecular weight (LMW) poly(I:C) were purchased from InvivoGen (San Diego, CA, USA).

Dual-luciferase reporter assay

To detect activation of the NF-κB pathway, 293T cells seeded in 24-well plates were co-transfected with the NF-κB firefly luciferase reporter (NF-κB-Luc), the internal control Renilla luciferase vector pCMV-RL, and plasmids expressing *I10L* or other relevant molecules. After 24 hours, cell lysates were prepared, and firefly and Renilla luciferase activities were analyzed using a dual-luciferase assay kit (Promega, Madison, WI, USA).

RNA extraction and Quantitative RT-PCR

Total RNA was extracted from PK-15 cells using an RNA extraction kit (BioFlux, Hangzhou, China) and reversed-transcribed into cDNA with a reverse transcription kit (Accurate Biology, Changsha, China) according to the manufacturer's protocols. The cDNA was used as a template for quantitative RT-PCR to investigate the effect of pI10L on the mRNA expression of porcine *ISG56*, *ISG54*, *IFN-β*, *IL6*, and *TNF-α* in PK-15 cells. All primer sequences are provided in Table 1.

Table 1
The primers used for qRT-PCR in this study.

Gene name	Sequence (5'→3')
Swine-*IFN-β*-F	5'-GATACCAACAAAGGAGCAGC-3'
Swine -*IFN-β*-R	5'-GAGCATCTCGTGGATAATCAATAC-3'
Swine -*Actin*-F	5'-TGAACCCCAAAGCCAACCGTGAG-3'
Swine -*Actin*-R	5'-AGTGGTGCGGCCAGAGGCGTACAGG-3'
Swine -*IL-6*-F	5'- AAGGTGATGCCACCTCAGAC-3'
Swine -*IL-6*-R	5'- TCTGCCAGTACCTCCTTGCT-3'
Swine -*ISG54*-F	5'-GGCAGAGAATGAAATGTGTGGGA-3'
Swine -*ISG54*-R	5'-AGAGGCAGGCGAGATAGGAGCAG-3'
Swine -*ISG56*-F	5'-CTTGGAGGAGATTGAGTTC-3'
Swine -*ISG56*-R	5'-ATACAGCCAGGCATAGTTG-3'
Swine -*TNF-α*-F	5'-CCACCAACGTTTTCCTCACT-3'
Swine -*TNF-α*-R	5'-CCCAGGTAGATGGGTTCGTA-3'
ASFV *I10L*-F	5'-TGCCACTACTGCTGATCTTCAA-3'
ASFV *I10L*-R	5'-TAACATTCTCCCGTTCCTCCTA-3'
ASFV *B646L*-F	5'-GCATCCCAGGGGATAAAATG-3'
ASFV *B646L*-R	5'-GAATAGGTTTGCTTTGGTGC-3'
ASFV *CP204L*-F	5'-AGGAGACGGAATCCTCAGCA-3'
ASFV *CP204L*-R	5'-GGGCTCTTGCTCAAACAACG-3'

Co-IP and Western blot analysis

293T cells were co-transfected with the indicated molecules for 24 hours. The cells were then lysed in 1% NP-40 lysis buffer [1% NP-40, 150 mM NaCl, 50 mM Tris-HCl (pH 8.0), 1 mM EDTA] supplemented with 1 mM phenylmethylsulfonyl fluoride (PMSF). The lysates were sonicated for 2 minutes and centrifuged at 10,000 rpm for 10 minutes at 4°C. The supernatants were incubated overnight at 4℃ with anti-Flag or anti-HA protein A/G agarose beads (Smart-Lifesciences, Changzhou, China) on a roller. The complexes were washed 6–8 times with ice-cold 1% NP-40 lysis buffer. The proteins were eluted by boiling in 2× SDS loading buffer [2% SDS, 10% glycerol, 60 mM Tris-HCl (pH 6.8), 5% β-mercaptoethanol, and 0.01% bromophenol blue], followed by Western blot analysis. For Western blot assay, the protein samples were separated by 7–12% sodium dodecyl sulfate polyacrylamide gel electrophoresis (SDS-PAGE) and transferred to a nitrocellulose membrane. The membrane was blocked for 1 hour in PBST

containing 3% milk and subsequently incubated with primary antibodies overnight at 4°C. After a 4-hour incubation with HRP-conjugated secondary antibody at 4°C, the immunoreactive bands were visualized by using an enhanced chemiluminescence (ECL) system.

GST pull-down assay

GST pull-down assays were performed as previously described [60]. Briefly, the pGEX-4T-1-pI10L and pET28a-His-TRAF6/MAVS plasmids were transformed into Escherichia coli BL21 cells. The cells were incubated with 1 mM IPTG for 6 hours at 37°C to induce protein expression. GST-I10L protein was incubated with glutathione-coated beads for 2 hours at 4°C, and His-TRAF6/MAVS protein was purified using a nickel affinity chromatography column. The purified His-TRAF6/MAVS protein was then mixed with GST or GST-I10L protein bound to glutathione-coated beads and incubated for 4–6 hours at 4°C. The beads were washed five times with lysis buffer, then treated with 2· SDS sample buffer, and subsequently analyzed by Western blotting.

Semidenaturing detergent agarose gel electrophoresis

The semidenaturing detergent agarose gel electrophoresis (SDD-AGE) was performed as previously described [14, 61]. Briefly, 293T cells were co-transfected with the indicated plasmids for 24 hours. Cells were then resuspended in crude mitochondria (P5) isolation buffer [10 mM Tris-HCl (pH 7.5), 10 mM KCl, 1.5 mM $MgCl_2$, 250 mM D-Mannitol] supplemented with 1 mM PMSF, and homogenized using a Dounce homogenizer to disrupt cell membranes. The cell lysates were centrifuged at 700·g for 10 minutes at 4℃ to remove cell fragments and nuclei. The supernatant was further centrifuged at 10000·g for 30 minutes at 4℃ to pellet the intact crude mitochondria. The crude mitochondria (P5) were lysed in 1× sample buffer (0.5× TBE, 10% glycerol, 2% SDS, and 0.0025% bromophenol blue) and loaded onto a 1.5% agarose gel (Bio-Froxx). Electrophoresis was performed in running buffer (1× TBE and 0.1% SDS) at a constant voltage of 100 V for 90 minutes at 4℃. Finally, proteins were transferred from the agarose gel onto a nitrocellulose filter membrane for subsequent Western blotting.

Small interfering RNA (siRNA) knockdown

siRNAs specifically targeting ASFV *I10L* were designed and synthesized by Beijing Tsingke Biotech Co (China). Primer PAMs were transfected with either negative control siRNA (siNC) or *I10L*-targeting siRNA (siI10L) by RNAiMax (Thermo Fisher Scientific, Waltham, MA, USA). The target sequences of ASFV *I10L* were 107-CAGATACGGATTGTAAGGA-125 and 262-GCCACTACTGCTGATCTTC-280. At 24 hours after siRNA transfection, the cells were infected with ASFV at a multiplicity of infection (MOI) of 1 for the indicated time points. The siRNA knockdown efficiency of *I10L* and mRNA expression levels of IFNs, ASFV p30, and p72 were measured by qRT-PCR. Protein expression levels of ASFV p30 and p72 were assessed by Western blotting. All ASFV infection experiments were performed in the animal biosafety level 3 (ABSL-3) of China Animal Health and Epidemiology center (CAHEC) approved by the Ministry of Agriculture and Rural Affairs (approval number 07140020201109-1).

siRNAs specifically targeting *MAVS* and *TRAF6* were designed and synthesized by Tsingke Biotech (Beijing, China). PK-15 cells were transfected with negative control siRNA (siNC), *MAVS*-targeting siRNA (siMAVS) or *TRAF6*-targeting siRNA (siTRAF6) using Mirus transfection reagent. At 24 hours after siRNA transfection, the cells were further transfected with ASFV *I10L* expression plasmid for an additional 24 hours, followed by transfection with poly(I:C) for 4 hours. The siRNA knockdown efficiency of *MAVS* and *TRAF6* was assessed by Western blotting, and the mRNA expression levels of *IFN-β* and *IL6* were measured by qRT-PCR. The target sequences of siMAVS, siTRAF6, and their negative control are listed in Table 2.

Table 2
siRNAs used in this study.

Oligo name		**Sequence (5'→3')**
siNC	Sense strand	UUCUCCGAACGUGUCACGU (dT) (dT)
	Antisense strand	ACGUGACACGUUCGGAGAA (dT) (dT)
siI10L-1	Sense strand	CAGAUACGGAUUGUAAGGA (dT) (dT)
	Antisense strand	UCCUUACAAUCCGUAUCUG (dT) (dT)
siI10L-2	Sense strand	GCCACUACUGCUGAUCUUC (dT) (dT)
	Antisense strand	GAAGAUCAGCAGUAGUGGC (dT) (dT)
siMAVS-1	Sense strand	CUGGUGCAAUGUCCACUAACG (dT) (dT)
	Antisense strand	CGUUAGUGGACAUUGCACCAG (dT) (dT)
siMAVS-2	Sense strand	CGAGUACGUGUCAGUGGAUAC (dT) (dT)
	Antisense strand	GUAUCCACUGACACGUACUCG (dT) (dT)
siTRAF6-1	Sense strand	GCAUCUUGAGGAUCAUCAA (dT) (dT)
	Antisense strand	UUGAUGAUCCUCAAGAUGC (dT) (dT)
siTRAF6-2	Sense strand	GGACAAAGUUGCAGAAAUA (dT) (dT)
	Antisense strand	UAUUUCUGCAACUUUGUCC (dT) (dT)

Statistical analysis

All experiments were performed at least three times unless otherwise indicated. Data are presented as the means ± standard deviations (SDs). Statistical significance between groups was determined using Student's t-test in GraphPad Prism 8.0 software (La Jolla, CA, USA). *$P < 0.05$, **$P < 0.01$, ***$P < 0.001$.

Declarations

Ethics approval and consent to participate

Not applicable.

Consent for publication

Not applicable.

Availability of data and materials

All data generated or analysed during this study are included in this published article.

Competing interests

The authors declare that they have no competing interests.

Fundings

This work was supported by the National Natural Science Foundation of China (NSFC) Projects of International Cooperation and Exchanges (W2412008), the Fundamental Research Funds for the Central Universities (KYCXJC2024005), the National Natural Science Foundation of China (U19A2039) and Kunlun Talents High-end Innovation and Entrepreneurship Talent Project of Qinghai Province.

Acknowledgments

All experiments on ASFV infection in this study were performed at the National/WOAH Reference Laboratory for African Swine Fever, located in China Animal Health and Epidemiology Center (CAHEC) in Shandong Province, China.

Author's contributions

Conceptualization was conceived by JNG, YSJ, XDW, and YJQ. JNG performed the experiments with help from JXL, HC, and XYG. Resources of this project were achieved from JNG, JXL, HC, YXH, SQG, JML, YSJ, XDW, and YJQ. Formal analysis and data curation was performed by JNG and YSJ. JNG wrote the original draft, and the manuscript was reviewed and edited by JNG, YSJ, and YJQ. YSJ, XDW, and YJQ supervised the entire project.

References

1. Teklue T, Sun Y, Abid M, Luo Y, Qiu HJ (2020) Current status and evolving approaches to African swine fever vaccine development. Transbound Emerg Dis 67(2):529–542
2. Dixon LK, Islam M, Nash R, Reis AL (2019) African swine fever virus evasion of host defences. Virus Res 266:25–33
3. Dixon LK, Chapman DA, Netherton CL, Upton C (2013) African swine fever virus replication and genomics. Virus Res 173(1):3–14

4. Blome S, Franzke K, Beer M (2020) African swine fever - A review of current knowledge. Virus Res 287:198099
5. Takeuchi O, Akira S (2010) Pattern Recognition Receptors and Inflammation. Cell 140(6):805–820
6. Beachboard DC, Horner SM (2016) Innate immune evasion strategies of DNA and RNA viruses. Curr Opin Microbiol 32:113–119
7. Kumar H, Kawai T, Akira S (2011) Pathogen Recognition by the Innate Immune System. Int Rev Immunol 30(1):16–34
8. Nie Y, Wang Y-Y (2013) Innate immune responses to DNA viruses. Protein Cel 4(1):1–7
9. Kato H, Takeuchi O, Sato S, Yoneyama M, Yamamoto M, Matsui K, Uematsu S, Jung A, Kawai T, Ishii KJ et al (2006) Differential roles of MDA5 and RIG-I helicases in the recognition of RNA viruses. Nature 441(7089):101–105
10. Nakhaei P, Genin P, Civas A, Hiscott J (2009) RIG-I-like receptors: Sensing and responding to RNA virus infection. Semin Immunol 21(4):215–222
11. Saito T, Gale M (2008) Differential recognition of double-stranded RNA by RIG-I–like receptors in antiviral immunity. J Exp Med 205(7):1523–1527
12. Chiu Y-H, MacMillan JB, Chen ZJ (2009) RNA Polymerase III Detects Cytosolic DNA and Induces Type I Interferons through the RIG-I Pathway. Cell 138(3):576–591
13. Xu L-G, Wang Y-Y, Han K-J, Li L-Y, Zhai Z, Shu H-B (2005) VISA Is an Adapter Protein Required for Virus-Triggered IFN-β Signaling. Mol Cell 19(6):727–740
14. Hou F, Sun L, Zheng H, Skaug B, Jiang Q-X, Chen Zhijian J (2011) MAVS Forms Functional Prion-like Aggregates to Activate and Propagate Antiviral Innate Immune Response. Cell 146(3):448–461
15. Zou PF, Tang JC, Li Y, Feng JJ, Zhang ZP, Wang YL (2021) MAVS splicing variants associated with TRAF3 and TRAF6 in NF-κB and IRF3 signaling pathway in large yellow croaker Larimichthys crocea. Dev Comp Immunol 121:104076
16. Belgnaoui SM, Paz S, Hiscott J (2011) Orchestrating the interferon antiviral response through the mitochondrial antiviral signaling (MAVS) adapter. Curr Opin Immunol 23(5):564–572
17. Jacobs JL, Coyne CB (2013) Mechanisms of MAVS Regulation at the Mitochondrial Membrane. J Mol Bio 425(24):5009–5019
18. Wu B, Hur S (2015) How RIG-I like receptors activate MAVS. Curr Opin Virol 12:91–98
19. Liu S, Cai X, Wu J, Cong Q, Chen X, Li T, Du F, Ren J, Wu Y-T, Grishin NV et al (2015) Phosphorylation of innate immune adaptor proteins MAVS, STING, and TRIF induces IRF3 activation. Science 347(6227):aaa2630
20. Levy DE, García-Sastre A (2001) The virus battles: IFN induction of the antiviral state and mechanisms of viral evasion. Cytokine Growth Factor Rev 12(2–3):143–156
21. Durbin JE, Fernandez-Sesma A, Lee CK, Rao TD, Frey AB, Moran TM, Vukmanovic S, García-Sastre A, Levy DE (2000) Type I IFN modulates innate and specific antiviral immunity. J Immunol (Baltimore Md: 1950) 164(8):4220–4228

22. Min Y, Kim MJ, Lee S, Chun E, Lee KY (2018) Inhibition of TRAF6 ubiquitin-ligase activity by PRDX1 leads to inhibition of NFKB activation and autophagy activation. Autophagy 14(8):1347–1358
23. Liu S, Chen J, Cai X, Wu J, Chen X, Wu YT, Sun L, Chen ZJ (2013) MAVS recruits multiple ubiquitin E3 ligases to activate antiviral signaling cascades. eLife 2:e00785
24. Deng L, Wang C, Spencer E, Yang L, Braun A, You J, Slaughter C, Pickart C, Chen ZJ (2000) Activation of the IkappaB kinase complex by TRAF6 requires a dimeric ubiquitin-conjugating enzyme complex and a unique polyubiquitin chain. Cell 103(2):351–361
25. Lamothe B, Besse A, Campos AD, Webster WK, Wu H, Darnay BG (2007) Site-specific Lys-63-linked tumor necrosis factor receptor-associated factor 6 auto-ubiquitination is a critical determinant of I kappa B kinase activation. J Biol Chem 282(6):4102–4112
26. Konno H, Yamamoto T, Yamazaki K, Gohda J, Akiyama T, Semba K, Goto H, Kato A, Yujiri T, Imai T et al (2009) TRAF6 establishes innate immune responses by activating NF-kappaB and IRF7 upon sensing cytosolic viral RNA and DNA. PLoS ONE 4(5):e5674
27. Kanayama A, Seth RB, Sun L, Ea CK, Hong M, Shaito A, Chiu YH, Deng L, Chen ZJ (2004) TAB2 and TAB3 activate the NF-kappaB pathway through binding to polyubiquitin chains. Mol Cell 15(4):535–548
28. Ran Y, Li D, Xiong MG, Liu HN, Feng T, Shi ZW, Li YH, Wu HN, Wang SY, Zheng HX et al (2022) African swine fever virus I267L acts as an important virulence factor by inhibiting RNA polymerase III-RIG-I-mediated innate immunity. PLoS Pathog 18(1):e1010270
29. Dodantenna N, Ranathunga L, Chathuranga WAG, Weerawardhana A, Cha JW, Subasinghe A, Gamage N, Haluwana DK, Kim Y, Jheong W et al (2022) African Swine Fever Virus EP364R and C129R Target Cyclic GMP-AMP To Inhibit the cGAS-STING Signaling Pathway. J Virol 96(15):e0102222
30. Yao M, Cao H, Li W, Hu Z, Rong Z, Yin M, Tian L, Hu D, Li X, Qian P (2024) African swine fever virus MGF505-6R attenuates type I interferon production by targeting STING for degradation. Front Immunol 15:1380220
31. Chen H, Yu Q, Gao X, Huang T, Bao C, Guo J, Wang Z, Lv J, Dai J, Babiuk LA et al (2025) ASFV pS183L protein negatively regulates RLR-mediated antiviral signalling by blocking MDA5 oligomerisation. Vet Res 56(1):70
32. Sun H, Yang J, Zhang Z, Wu M, Tian Z, Liu Y, Zhang X, Zhong J, Yang S, Chen Y et al (2025) The African swine fever virus gene MGF_360-4L inhibits interferon signaling by recruiting mitochondrial selective autophagy receptor SQSTM1 degrading MDA5 antagonizing innate immune responses. mBio 16(4):e0267724
33. Zhao J, Mou C, Zhu L, Sun X, Chen Z (2025) African swine fever virus-encoded pE248R protein inhibits interferon production via blocking RIG-I-mediated antiviral signaling. Int J Biol Macromol 327(Pt 1):147383
34. Chen H, Wang Z, Gao X, Lv J, Hu Y, Jung YS, Zhu S, Wu X, Qian Y, Dai J (2022) ASFV pD345L protein negatively regulates NF-κB signalling by inhibiting IKK kinase activity. Vet Res 53(1):32

35. Revilla Y, Granja AG (2009) Viral Mechanisms Involved in the Transcriptional CBP/p300 Regulation of Inflammatory and Immune Responses. Crit Rev Immunol 29(2):131–154
36. Liu W, Yang L, Di C, Sun J, Liu P, Liu H (2024) Nonstructural Protein A238L of the African Swine Fever Virus (ASFV) Enhances Antiviral Immune Responses by Activating the TBK1-IRF3 Pathway. Veterinary Sci 11(6)
37. Vydelingum S, Baylis SA, Bristow C, Smith GL, Dixon LK (1993) Duplicated genes within the variable right end of the genome of a pathogenic isolate of African swine fever virus. J Gen Virol 74(10):2125–2130
38. Chen X, Li LF, Yang ZY, Li M, Fan S, Shi LF, Ren ZY, Cao XJ, Zhang Y, Han S et al (2023) The African swine fever virus I10L protein inhibits the NF-κB signaling pathway by targeting IKKβ. J Virol 97(9):e0056923
39. Deng J, Zheng Y, Zheng SN, Nan ML, Han L, Zhang J, Jin Y, Pan JA, Gao C, Wang PH (2023) SARS-CoV-2 NSP7 inhibits type I and III IFN production by targeting the RIG-I/MDA5, TRIF, and STING signaling pathways. J Med Virol 95(3)
40. Yin Q, Lin S-C, Lamothe B, Lu M, Lo Y-C, Hura G, Zheng L, Rich RL, Campos AD, Myszka DG et al (2009) E2 interaction and dimerization in the crystal structure of TRAF6. Nat Struct Mol Biol 16(6):658–666
41. Yamamoto M, Gohda J, Akiyama T, Inoue JI (2021) TNF receptor-associated factor 6 (TRAF6) plays crucial roles in multiple biological systems through polyubiquitination-mediated NF-κB activation. *Proceedings of the Japan Academy Series B, Physical and biological sciences* 97(4):145–160
42. Ren Z, Ding T, Zuo Z, Xu Z, Deng J, Wei Z (2020) Regulation of MAVS Expression and Signaling Function in the Antiviral Innate Immune Response. Front Immunol 11
43. Mao A-P, Li S, Zhong B, Li Y, Yan J, Li Q, Teng C, Shu H-B (2010) Virus-triggered Ubiquitination of TRAF3/6 by cIAP1/2 Is Essential for Induction of Interferon-β (IFN-β) and Cellular Antiviral Response. J Biol Chem 285(13):9470–9476
44. Seth RB, Sun L, Ea CK, Chen ZJ (2005) Identification and characterization of MAVS, a mitochondrial antiviral signaling protein that activates NF-kappaB and IRF 3. Cell 122(5):669–682
45. Tang ED, Wang CY (2009) MAVS self-association mediates antiviral innate immune signaling. J Virol 83(8):3420–3428
46. Deshaies RJ, Joazeiro CAP (2009) RING Domain E3 Ubiquitin Ligases. Annu Rev Biochem 78:399–434
47. Park HH (2018) Structure of TRAF Family: Current Understanding of Receptor Recognition. Front Immunol 9
48. Kong QZ, Guo LT, Yang JN, Wang YF, Zhao JX, Kong SH, Zhang M, Yan S, Jin Y (2016) Anti-Inflammatory Effects of TRAF-Interacting Protein in Rheumatoid Arthritis Fibroblast-Like Synoviocytes. *Mediators of inflammation* 2016:3906108
49. Luo XB, Xi JC, Liu Z, Long Y, Li LT, Luo ZP, Liu DH (2020) Proinflammatory Effects of Ubiquitin-Specific Protease 5 (USP5) in Rheumatoid Arthritis Fibroblast-Like Synoviocytes. *Mediators of*

inflammation 2020:8295149

50. Summerfield A (2012) Viewpoint: Factors involved in type I interferon responses during porcine virus infections. Vet Immunol Immunopathol 148(1–2):168–171
51. Ivashkiv LB, Donlin LT (2014) Regulation of type I interferon responses. Nat Rev Immunol 14(1):36–49
52. Chen Y, Shi Y, Wu J, Qi N (2021) MAVS: A Two-Sided CARD Mediating Antiviral Innate Immune Signaling and Regulating Immune Homeostasis. Front Microbiol 12:744348
53. Zhou D, Li Q, Jia F, Zhang L, Wan S, Li Y, Song Y, Chen H, Cao S, Ye J The Japanese Encephalitis Virus NS1' Protein Inhibits Type I IFN Production by Targeting MAVS. *Journal of immunology (Baltimore, Md*: (1950)) 2020, 204(5):1287–1298) 2020, 204(5):1287–1298
54. Ekanayaka P, Lee BH, Weerawardhana A, Chathuranga K, Park JH, Lee JS (2021) Inhibition of MAVS Aggregation-Mediated Type-I Interferon Signaling by Foot-and-Mouth Disease Virus VP3. Viruses 13(9)
55. Shi Y, Yuan B, Qi N, Zhu W, Su J, Li X, Qi P, Zhang D, Hou F (2015) An autoinhibitory mechanism modulates MAVS activity in antiviral innate immune response. Nat Commun 6:7811
56. Qi N, Shi Y, Zhang R, Zhu W, Yuan B, Li X, Wang C, Zhang X, Hou F (2017) Multiple truncated isoforms of MAVS prevent its spontaneous aggregation in antiviral innate immune signalling. Nat Commun 8:15676
57. Paz S, Vilasco M, Werden SJ, Arguello M, Joseph-Pillai D, Zhao T, Nguyen TL, Sun Q, Meurs EF, Lin R et al (2011) A functional C-terminal TRAF3-binding site in MAVS participates in positive and negative regulation of the IFN antiviral response. Cell Res 21(6):895–910
58. Brenke JK, Popowicz GM, Schorpp K, Rothenaigner I, Roesner M, Meininger I, Kalinski C, Ringelstetter L, R'kyek O, Jürjens G et al (2018) Targeting TRAF6 E3 ligase activity with a small-molecule inhibitor combats autoimmunity. J Biol Chem 293(34):13191–13203
59. Bo Z, Miao Y, Xi R, Zhong Q, Bao C, Chen H, Sun L, Qian Y, Jung YS, Dai J (2020) PRV UL13 inhibits cGAS-STING-mediated IFN-β production by phosphorylating IRF3. Vet Res 51(1):118
60. Chen H, Qian Y, Chen X, Ruan Z, Ye Y, Chen H, Babiuk LA, Jung YS, Dai J (2019) HDAC6 Restricts Influenza A Virus by Deacetylation of the RNA Polymerase PA Subunit. J Virol 93(4)
61. Hou J, Han L, Zhao Z, Liu H, Zhang L, Ma C, Yi F, Liu B, Zheng Y, Gao C (2021) USP18 positively regulates innate antiviral immunity by promoting K63-linked polyubiquitination of MAVS. Nat Commun 12(1):2970

Figures

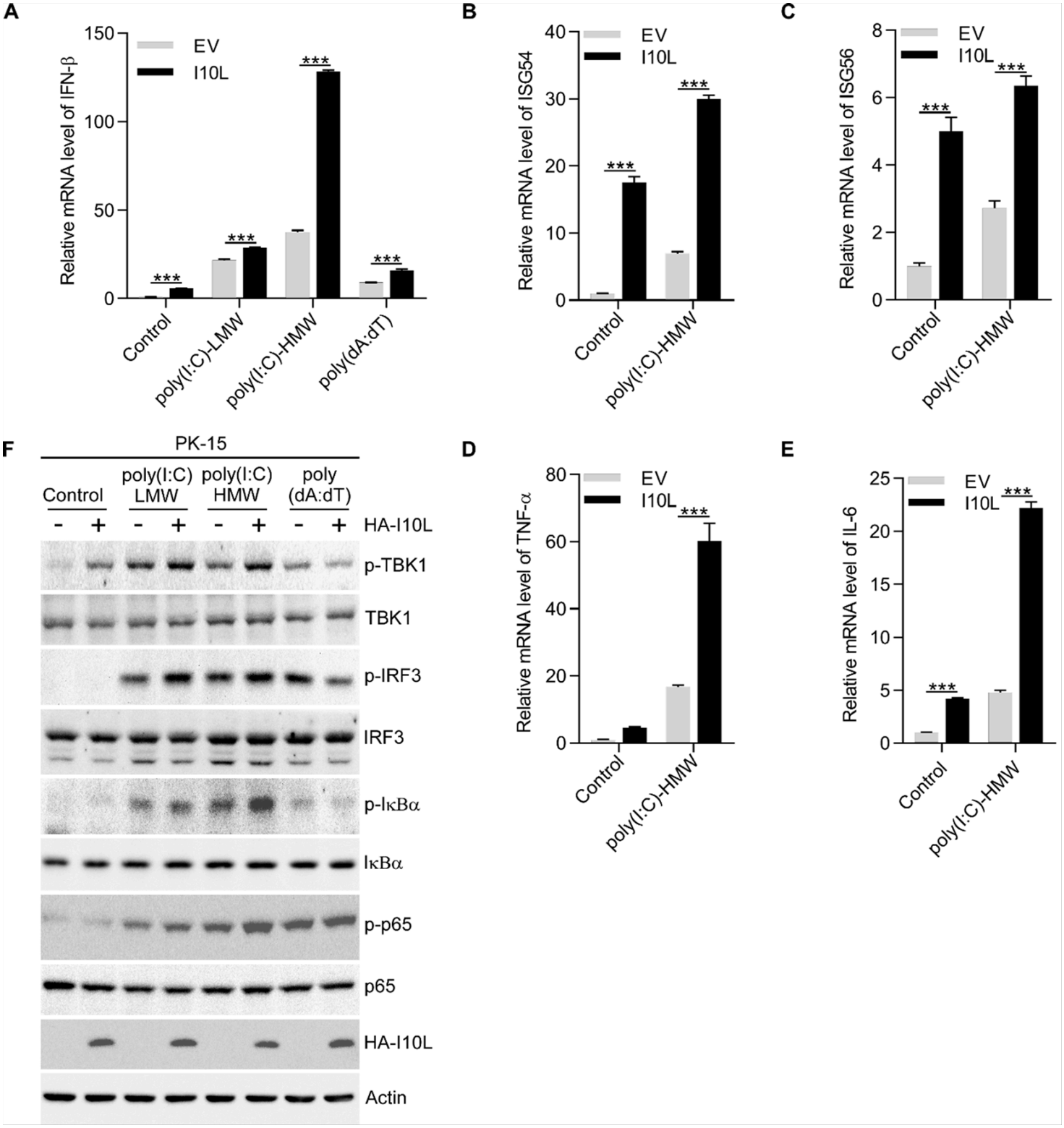


Figure 1

ASFV pI10L promotes poly(I:C)-mediated antiviral genes production. (A-E) ASFV pI10L promotes poly(I:C)-triggered transcription of antiviral genes in PK-15 cells. PK-15 cells were transfected with empty vector or HA-tagged pI10L (1 mg) for 24 hours and then transfected with poly(I:C)-LMW/HMW (2 mg/mL) or poly(dA:dT) (2 mg/mL)for another 2 hours, followed by qRT-PCR analysis of the *IFN-b*, *TNF-a*, *IL6*, *ISG54*, and *ISG56*genes. (F) ASFV pI10L promotes poly(I:C)-triggered the phosphorylation of

downstream signaling molecules in PK-15 cells. PK-15 cells were transfected with the empty vector or HA-tagged pI10L (1 mg) for 24 hours, and then transfected with poly(I:C)-LMW/HMW (2 mg/mL) or poly(dA:dT) (2 mg/mL) for an additional 3 hours, followed by Western blot analysis.

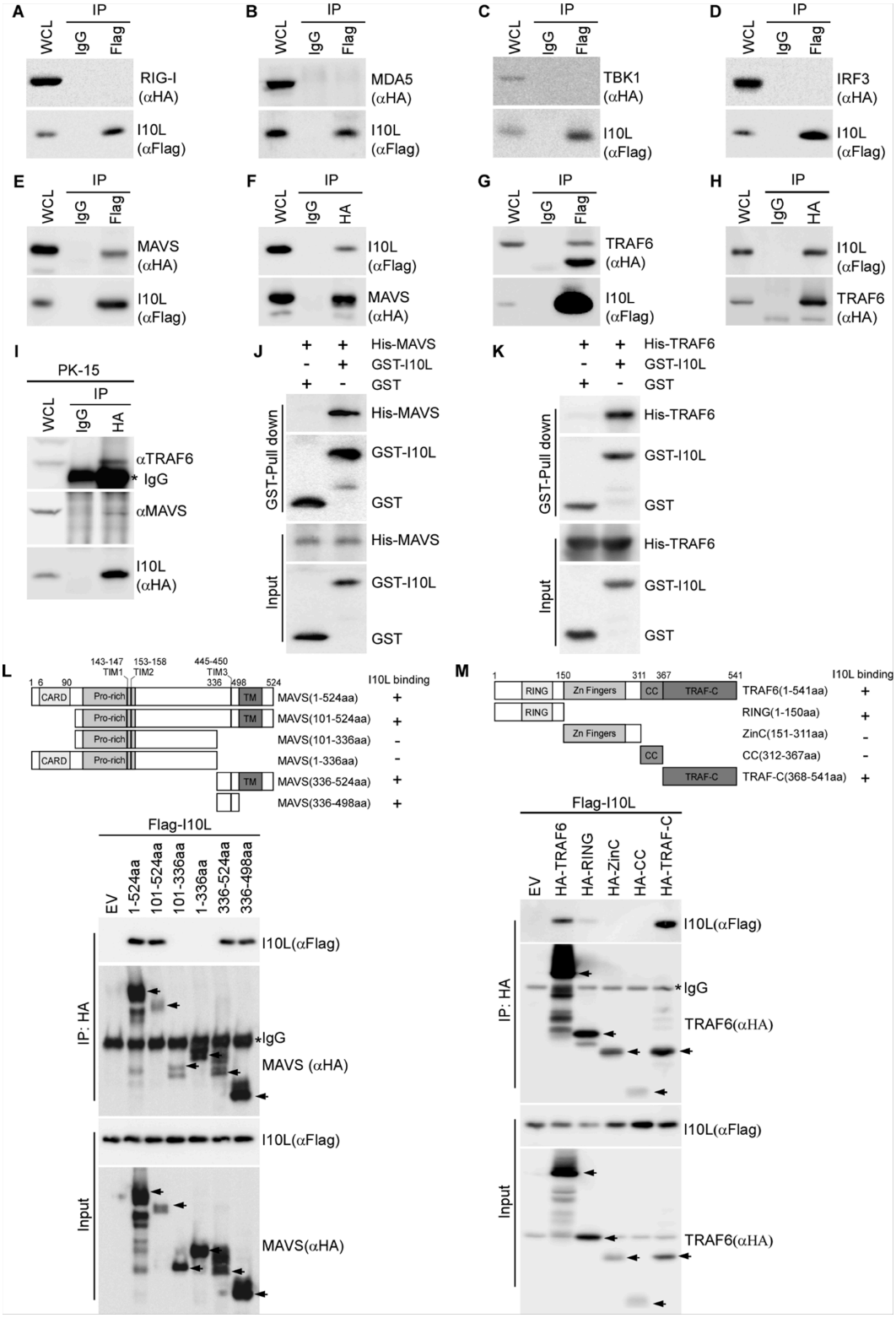


Figure 2

ASFV pI10L interacts with MAVS and TRAF6. (A-H) ASFV pI10L interacts with MAVS and TRAF6. 293T cells were co-transfected with the *I10L*-expressing plasmid and the plasmids encoding HA-tagged RIG-I, MDA5, MAVS, TBK1, TRAF6, IRF3 for 24 hours. The cells were then harvested and lysed, and the lysates were incubated with protein A/G agarose beads and either the indicated antibodies or nonspecific IgG, followed by Western blot analysis. (I) ASFV pI10L interacts with endogenous MAVS and TRAF6. The PK-15 cells were transfected with the *I10L*-expressing plasmid for 24 hours and then transfected with poly(I:C)-HMW (2 mg/mL) for another 6 hours. The cells were lysed and immunoprecipitated with anti-HA antibody and control IgG, followed by Western blot analysis. Asterisk indicates nonspecific bands. (J and K) ASFV pI10L binds to MAVS and TRAF6 in vitro. GST or GST-tagged pI10L was incubated with the His-tagged MAVS and His-tagged TRAF6, followed by Western blot analysis. (L) ASFV pI10L interacts with the C-terminal region of MAVS. HA-MAVS and each its truncation mutants were co-transfected with Flag-pI10L in 293T cells for 24 hours. Cell lysates were immunoprecipitated with an anti-HA antibody and then analyzed by Western blot. (M) ASFV pI10L interacts with the RING or TRAF-C domains of TRAF6. HA-TRAF6 and each its truncation mutants were co-transfected with Flag-pI10L in 293T cells for 24 hours. Cell lysates were immunoprecipitated with an anti-HA antibody and then analyzed by Western blot.

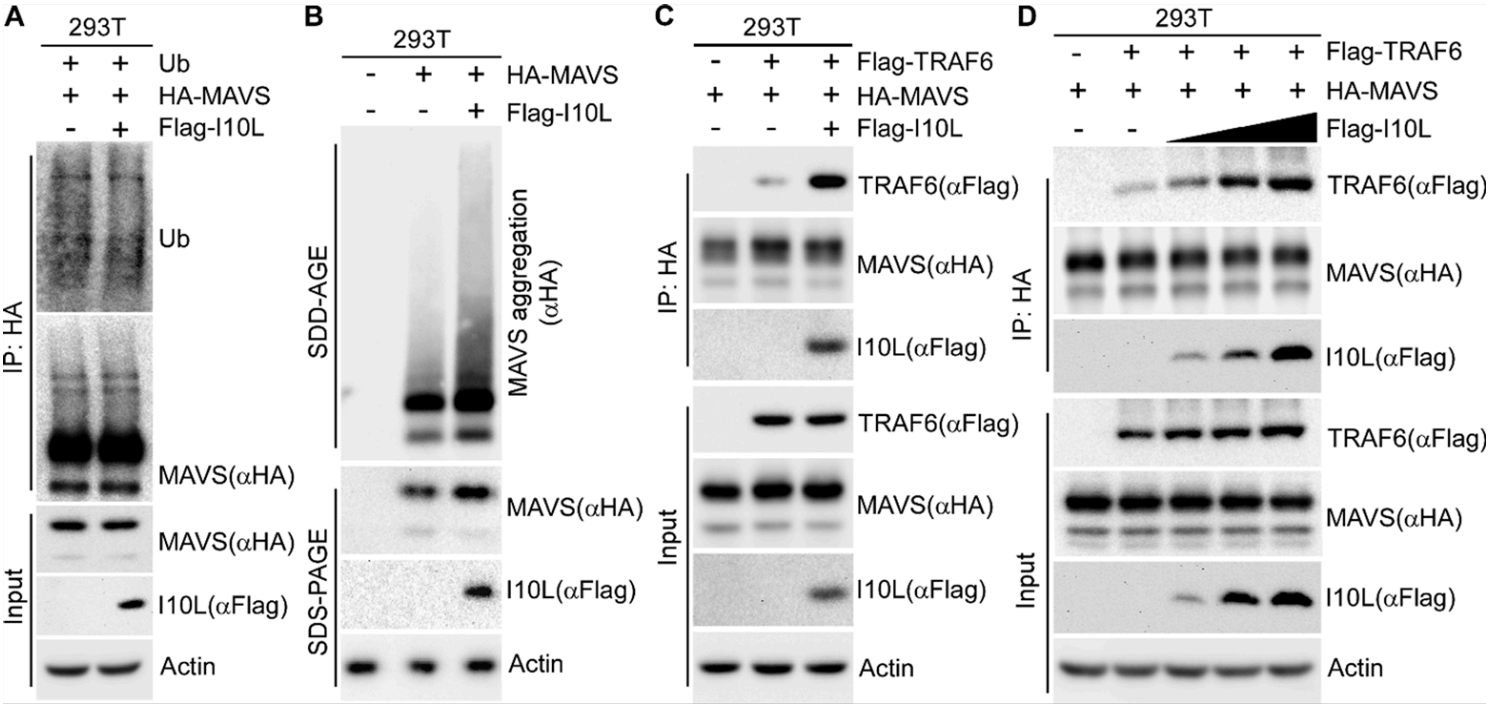


Figure 3

ASFV pI10L promotes MAVS aggregation and the recruitment of downstream components. (A) The ASFV pI10L does not affect the ubiquitination of MAVS. 293T cells were co-transfected with the HA-MAVS, Flag-pI10L, and Ub-expressing plasmids for 24 hours. Cell lysates were immunoprecipitated with an anti-HA antibody and then analyzed by Western blot. (B) ASFV pI10L promotes MAVS aggregation. 293T cells were co-transfected with empty vector or Flag-pI10L and HA-MAVS for 24 hours. The cells were harvested, crude mitochondria were isolated, and subjected to SDD-AGE (top). Whole-cell lysates

were analyzed by SDS-PAGE (bottom). (C and D) ASFV pI10L promotes the interaction between MAVS and TRAF6 in a dose-dependent manner. 293T cells were co-transfected with Flag-TRAF6 (1.5 mg), HA-MAVS (0.5 mg) and empty vector or increasing amounts of Flag-pI10L (0.25, 0.5, and 1 mg) for 24 hours. Cell lysates were immunoprecipitated with ananti-HA antibody and then analyzed by Western blot.

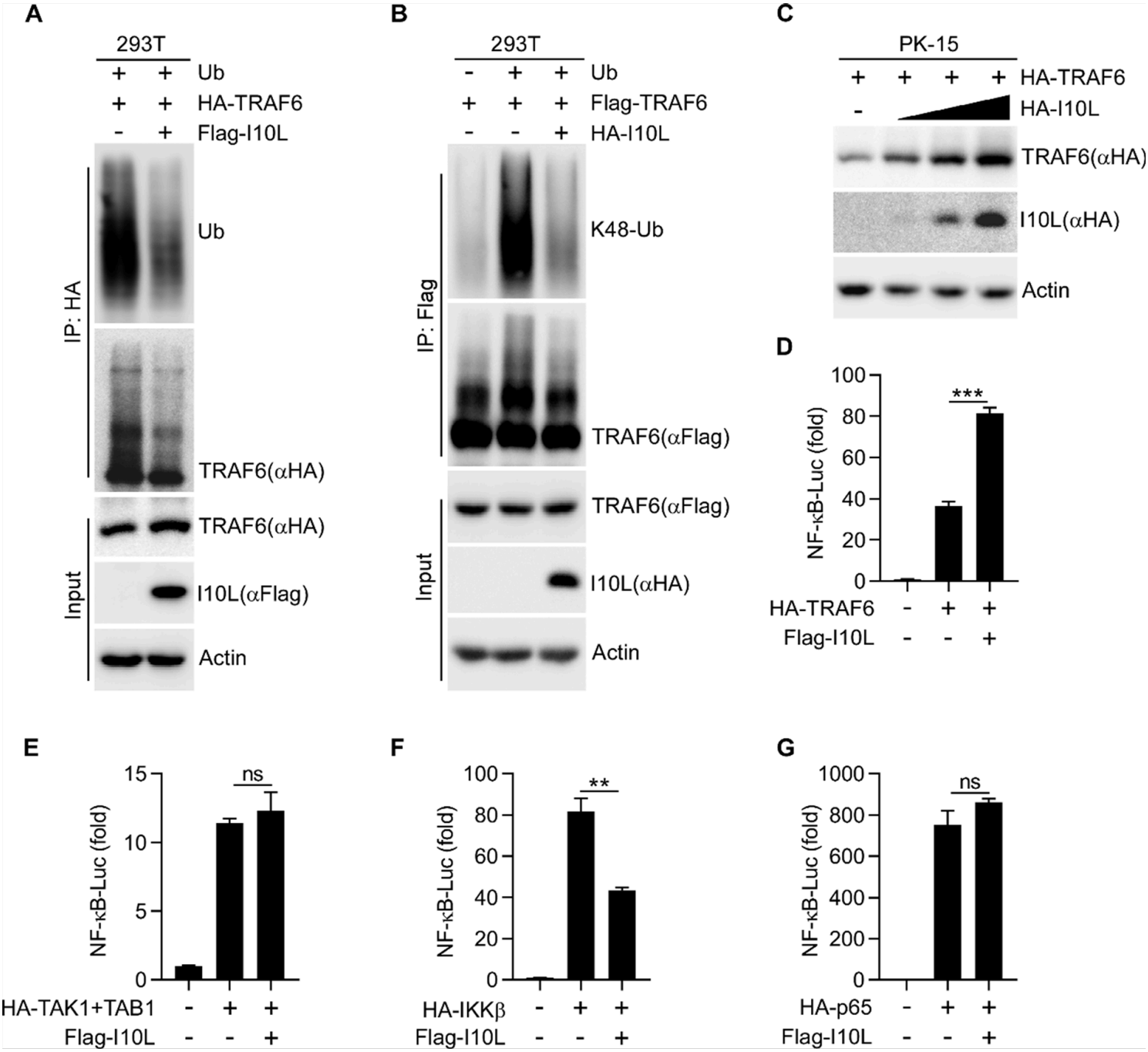


Figure 4

ASFV pI10L inhibits TRAF6 polyubiquitination and stabilizes TRAF6 protein. (A) ASFV pI10L inhibits the ubiquitination of TRAF6. 293T cells were co-transfected with the HA-TRAF6, Flag-pI10L, and Ub-expressing plasmids for 24 hours. Cell lysates were immunoprecipitated with an anti-HA antibody and then analyzed by Western blot. (B) ASFV pI10L inhibits the K48-linked ubiquitination of TRAF6. (C)

Overexpression of pI10L increased exogenous TRAF6 levels in a dose-dependent manner. PK-15 cells were transfected with HA-TRAF6 (0.8 mg) and varying doses of HA-pI10L (0.2, 0.4, and 0.8 mg) plasmids, followed by Western blot analysis. (D-G) ASFV pI10L promotes the NF-κB activation by targeting TRAF6. 293T cells were transfected with an NF-kB-Luc reporter and a pCMV-RL reporter, the plasmids expressing HA-TRAF6 (D), HA-TAK1 andHA-TAB1 (E), HA-IKKb(F), or HA-p65(G), together with Flag-pI10L plasmids for 24 hours, followed by luciferase assay.

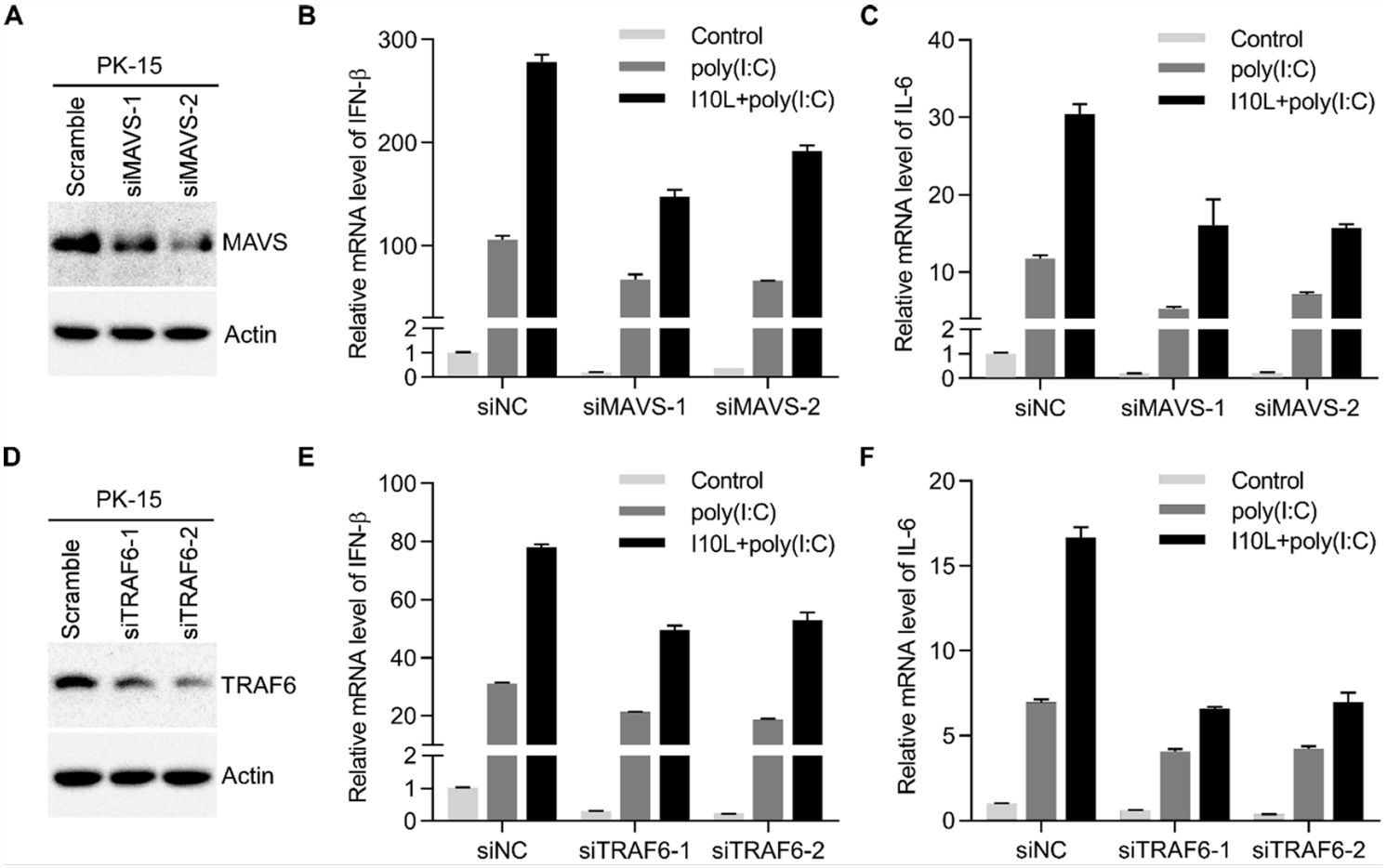


Figure 5

Knockdown of *MAVS*or *TRAF6* reduces pI10L-mediated promotion of antiviral genes production. (A and D) The knockdown efficiency of MAVS and TRAF6. PK-15 cells were transfected with 50 nM of siNCs or siRNAs targeting *MAVS* or *TRAF6* for 48 hours. The interference efficiency was assessed by Western blot analysis with anti-MAVS or anti-TRAF6 antibodies. (B, C, E, and F) Knockdown of *MAVS*or *TRAF6* downregulates pI10L-mediated promotion of IFN-b and IL-6 production. PK-15 cells were transfected with 50 nM of siNCs, siMAVS-1, siMAVS-2, siTRAF6-1, or siTRAF6-2. After 24 hours, cells were transfected with HA-tagged pI10L plasmids for an additional 24 hours, then stimulated with poly(I:C)-HMW (2 mg/mL) for another 4 hours. The mRNA levels of *IFN-b*, *IL6* were measured by qRT-PCR assay.

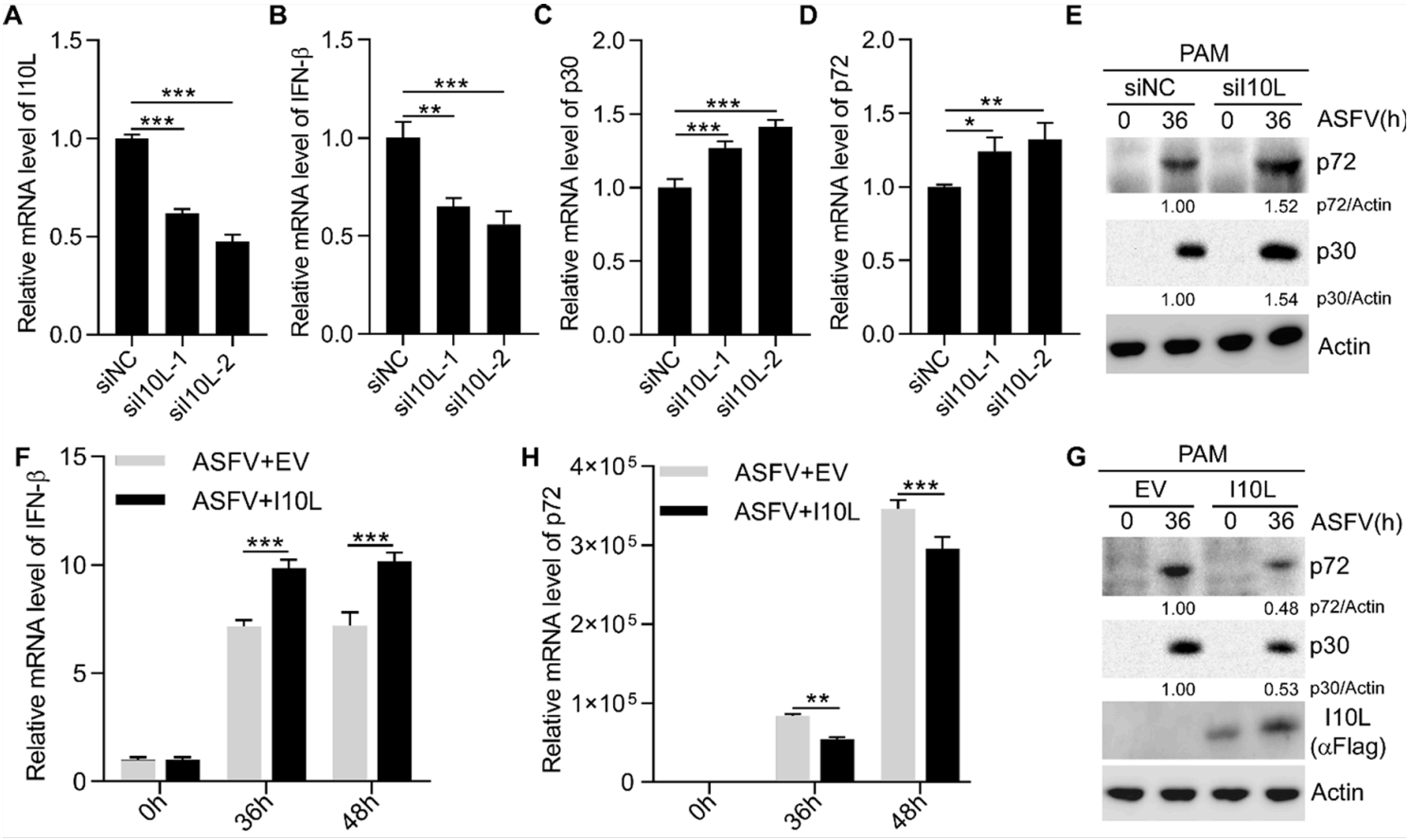


Figure 6

Knockdown of *I10L* enhances ASFV replication and reduces ASFV-induced antiviral response. (A-D) PAM cells were transfected with siNCs or siRNAs targeting *I10L* for 24 hours. The cells were then infected with ASFV (1 MOI) for 36 hours. The mRNA levels of *I10L*, *IFN-b*, p72,and p30 were determined by qRT-PCR assay. (E) PAM cells were transfected with siNCs or siRNAs targeting *I10L* for 24 hours and then infected with ASFV (1 MOI) for 36 hours. The expression of p72 and p30 proteins wasdetected by Western blot. (F and G) PAM cells were transfected with the *I10L*-expressing plasmids or empty vector for 24 hours, and then infected with ASFV (1 MOI) for 36 or 48 hours. The mRNA levels of *IFN-b* and p72 were measured by qRT-PCR assay. (H) PAM cells were transfected with the *I10L*-expressing plasmids or empty vector for 24 hours and then infected with ASFV (1 MOI) for 36 hours. The expression of Flag-pI10L, p72, and p30 proteins wasdetected by Western blot.

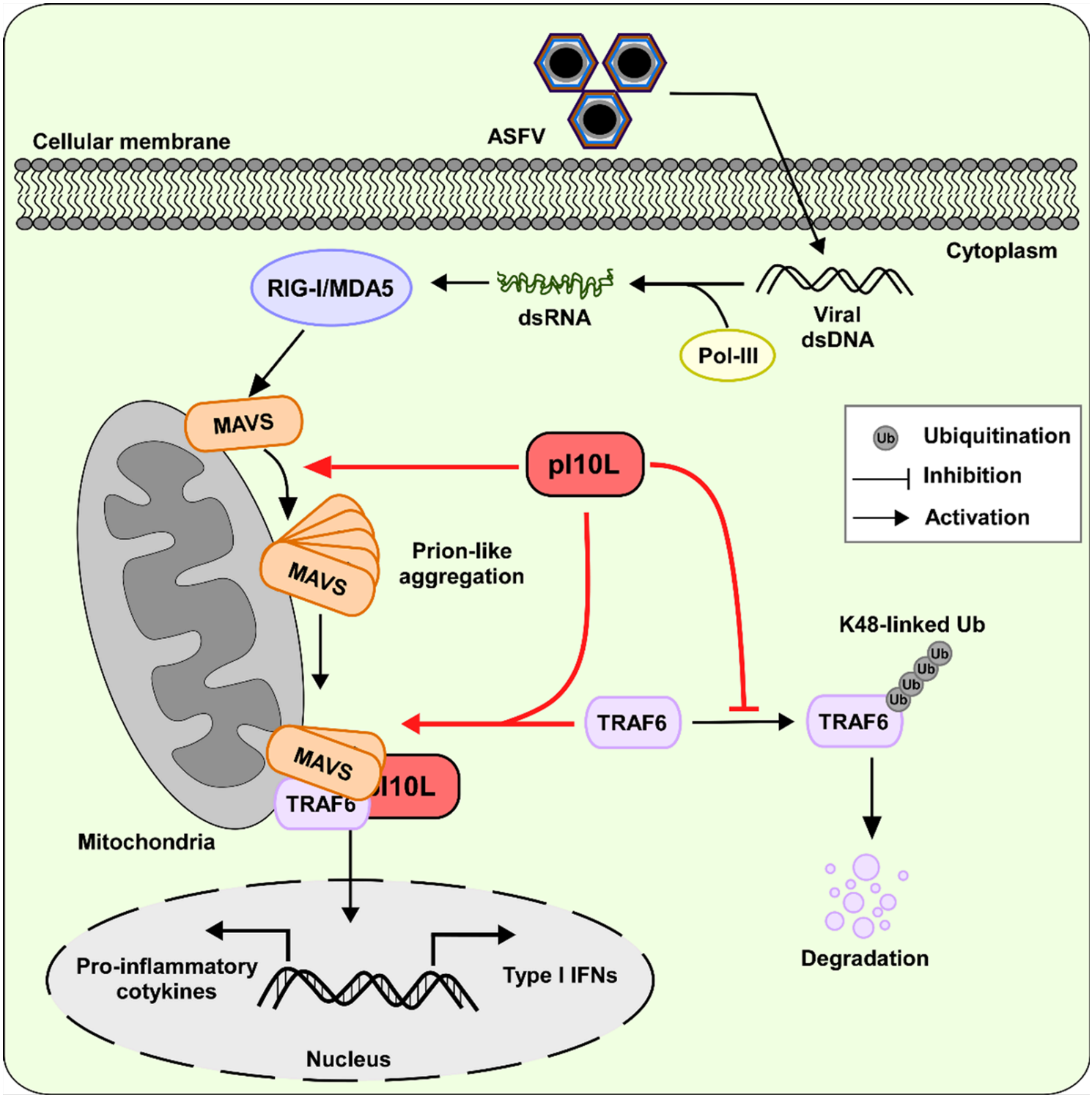


Figure 7

Model of the molecular mechanism for pI10L to promote type I IFN production. Upon infection, ASFV expresses the pI10L. pI10L interacts with MAVS,promotingMAVS aggregation and the recruitment of downstream TRAF6, thereby facilitating the innate antiviral response. Additionally, ASFV pI10L targets TRAF6 and inhibits its K48-linked polyubiquitination, contributingto increasing TRAF6 accumulation and promoting TRAF6-mediated activation of the NF-kB signaling pathway.